2019 SAUPEC/RobMech/PRASA Conference
Bloemfontein, South Africa, January 28-30, 2019

Dynamic load-shedding for enhancement of power system stability for the Lesotho 132 kV transmission network

Ikaneng Victor Raphoolo
School of Electrical, Electronic and Computer Engineering
North-West University
Potchefstroom, South Africa
raphooloi@electromech.co.ls

Jan A. de Kock
School of Electrical, Electronic and Computer Engineering
North-West University
Potchefstroom, South Africa
jan.dekock@nwu.ac.za

ABSTRACT

The transient and dynamic stability are key elements that a system should satisfy to achieve stable system operation [1]. Fault type and location determine the impact that each fault puts on the system and whether power generators stay in synchronism. The Eskom-Mabote tie-line is key to satisfying Lesotho power system (LPS) peak load demand of 150 MW. Any faults on the tie-line that affect the power transfer capacity threaten the continuity of supply as they can result in system collapse. When clearing of faults is longer than the critical fault clearing time (CFCT), the generators lose synchronism and trip as a protective measure. The knock-on effect of system collapse contributes to Lesotho's struggling techno-economic standing.

The absence of a contingency to counteract the effects of the tie-line failure and so minimize the impact on the supply/demand mismatch, often results in frequency violations. Using DIgSILENT, this study investigates the impact of the tie-line failure during the peak load and proposes load curtailment measures by employing dynamic-load shedding to avoid complete system collapse. Secondly, the study outlines the solutions to overcome the existing supply/demand challenge during tie-line failure to minimize the recurrence of system collapse. Thirdly, the study investigates the causes of failure to resynchronize and the impact of live system load to satisfy the requisite resynchronizing requirements, viz. change in voltage, frequency, and load angle. The study also reflects on the impact of different amounts of live loads during restoration considering the hypothetical extreme cases.

Keywords—power system stability, dynamic load-shedding, critical fault clearing time, tie-line, system collapse

I. INTRODUCTION

In 1998, the load demand on the LPS was below 72 MW, in 2013 the peak load demand increased to 126 MW. This development has increased the need for dynamic load-shedding on the system during perturbations on the tie-line. This study conducts investigation only on the faults that caused large impacts, such as a severe three-phase fault, on the tie-line. Taking for instance the fault that caused the 50 km Tweespruit-Eskom Maseru Bulk (EMB) 132 kV transmission line to trip resulting in a power transfer deficit and causing a system collapse because of frequency violations.

To circumvent a complete blackout, the study applies a staged system loading permitting approximately 64 MW live load. The determinations for dropping the loads consider the load on the generating units together with the requisite operating reserve and corresponding system losses.

Clearing of the faults on the tie-line occurs in the normal zone 1 and zone 2 protection times of 0.0 s and 0.5 s respectively. Zones 1 and 2 protection cover 80% and 120% of the protected line length respectively. Simulations for determining the critical fault clearing time (CFCT) of 0.34 s, considered a severe three-phase fault on the tie-line for a fault on line 1 when line 2 was in-service. Bearing in mind the CFCT and the typical zones 1 and 2 protection operation times, the three-phase fault undoubtably caused loss of transient stability on the generating units.

Recently, upon re-closing the tie-line breaker, the system saw failure in resynchronizing. The requisite conditions for resynchronization are published in [1] and [2], this study however deviates from IEEE Std C50.13 of 2014 [3, p. 15] in that the resynchronizing was possible when the system load was increased to 112.3%, breaker load angle increased to 10.76°, and frequency varied up to 0.6 Hz.

II. THE SYSTEM MODELING APPROACH

A. The 2013 system load model

The system load that this study makes use of originates from actual 30 minutes data measured from all the Lesotho Electricity Company (LEC) substations and afterward compressing the load using moving average toolbox in Microsoft Excel (see 111111Eq.1111)111 to achieve overall smooth trends in Fig. 1.

$$F_t = \frac{A_r + A_{t-1} + \cdots \ldots A_{t-n+1}}{n} \quad (1)$$

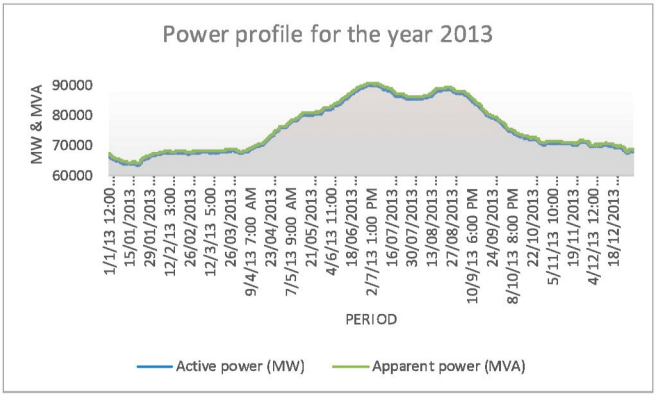

Fig. 1: The active and apparent power profile- July 2013

Taking July 2013, the peak load occurred between 08:00 and 09:00. The load profile indicates no direct relationship between active power and reactive power consumed. The data shows that the increase in active power consumed was not

978-1-7281-0369-3/19/$31.00 ©2019 IEEE

directly proportional to the reactive power consumption. To represent the system peak load of 150 MW recorded in 2016, the load was increased proportionally on all substations.

Noteworthy is that another set of data provided by LEC in the form of monthly consumption summary for 2017 indicates a reduced peak demand of 118 MW.

B. *Voltage and frequency dependency of loads*

The study determined the load composition to be neither static nor dynamic hence the adoption of complexed load model to represent the load combination. The simulations adopted the DIgSILENT values of 1.6 *kpu* and 1.8 *kpu* considering a three-phase load [4]. From reference [4], the Eq. (2), (3) and (4) mathematically express the static and dynamic loads respectively.

$$P = P_0 \left(\frac{v}{v_0}\right)^{kpu} * \left(1 + k_{pf}\left(\frac{\Delta f}{f_0}\right)\right) \quad (2)$$

$$Q = Q_0 \left(\frac{v}{v_0}\right)^{kpu} * \left(1 + k_{pf}\left(\frac{\Delta f}{f_0}\right)\right) \quad (3)$$

$$t_e = \left[\frac{T_{mo}}{100}\right]\left[\frac{v^2}{v_0^2}\right]\left[\frac{s}{s_0}\right]\left[\frac{s_0^2+s_{cr}^2}{s^2+s_{cr}^2}\right] \quad (4)$$

C. *The grid model*

The model used the external grid as a voltage source that has impedance to represent the physical characteristics. The acceleration time constant represented the combined inertia for all the connected systems [4].

D. *The hydro-generators' model*

The 'Muela hydro-power is rated 96 *MVA*, it uses the synchronous generators to covert the mechanical energy to electrical energy. To characterize the generator's behavior during dynamic conditions, the model used the gov_Hygov, IEEET1 and PSS2A to model the governor, automatic voltage regulator (*AVR*) and power system stabilizer (*PSS*) respectively.

E. *The transmission line model*

The Lesotho transmission and distribution system consists of mostly two winding (132/33 *kV*) and few three-winding (132/66/11 *kV*) transformers. The model used a detailed transformer model that included on-load tap changers to control voltage, phase angle or both etc. [5].

F. *The Overhead lines model*

The longest transmission line is less than 80 km, not transposed, and thus falls within the short line category [4]. The model used the standard DIgSILENT overhead line data for load-flow and RMS simulations, and still achieved reasonable results. The conductors used in the model are 'bear' for 132 *kV* and 'panther' for 33 *kV* lines.

III. THE CAUSE AND EFFECT OF PERTURBATIONS ON ESKOM TIE-LINE

When the tie-line trips, the constraint for continued supply of power is the 96 MVA installed generating units. With no dynamic load-shedding scheme, the system collapses because of frequency violations resulting from the mismatch in supply/ demand. The computations for establishing the total load to be shed allowed 8 MW [5] [6] for spinning reserve to meet Southern African Power Pool (SAPP) operational requirements and 4.87 MW system losses (for the LPS only).

In the past five years, LPS experienced various blackout conditions including the 8th May 2016 and 16th March 2018 incidents. This study used two hypothetical study cases, i.e. busbar faults on Tweespruit substation with and without dynamic load-shedding to examine the system behaviour during events that caused power transfer failure to the LPS.

A. *Busbar faults in Tweespruit substation – No dynamic load-shedding application*

On application of a three-phase fault on the busbars at Tweespruit substation, the protection operation resulted in power transfer failure on the tie-line. The system collapsed because of frequency violations (see Fig. 2). Other system violations included the generator loading and voltage.

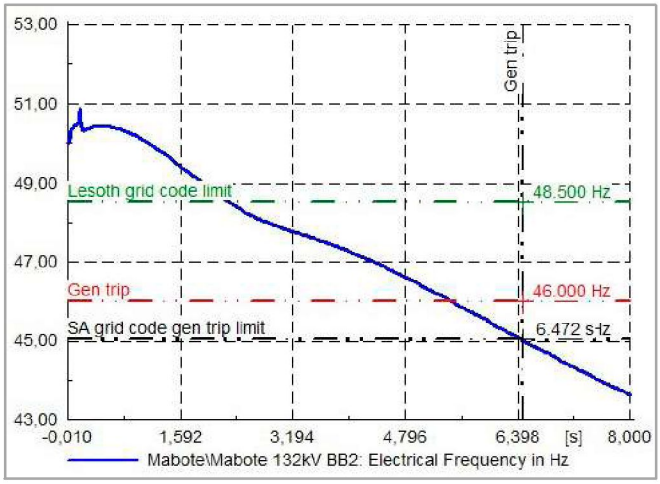

Fig. 2: The frequency characteristics during faulted condition at Tweespruit substation

B. *Busbar faults on Tweespruit substation – with dynamic load-shedding application*

To prevent system collapse, various combinations of loads were tripped during stage 1 ranging from 73.17 MW to 46.72 MW to evaluate the impact on the system for the least to most effective combination for optimal results (see Table 1).

Table 1: Different amounts of loads tripped for different study cases

Stage	Cumulative value of load-shed per stage							
	Case 1	*Case 2*	*Case 3*	*Case 4*	*Case 5*	*Case 6*	*Case 7*	*Case 8*
1	73,17	67,51	64,72	64,72	64,72	57,25	49,15	46,72
2	86,86	88,49	87,75	74,57	74,57	59,48	65,46	76,25
3	93,52	90,55	89,81	89,81	85,36	63,33	72,19	80,25
4	-	-	-	-	89,21	77,85	76,25	-
5	-	-	-	-	-	81,21	80,25	-

The determining factor during the dynamic load-shedding was the generators' loading together with the frequency deviation using the South African grid code as a guide. The load-shedding operations considered the different study cases to assess the system response. The success of the operation depended on tripping the substations that connect directly to

Mabote substation (see Fig. 3), because of its location, for stage 1 while the succeeding stages were a combination of loads excluding the manufacturing sector and Central Business Districts (CBDs) to mention a few essential load centers.

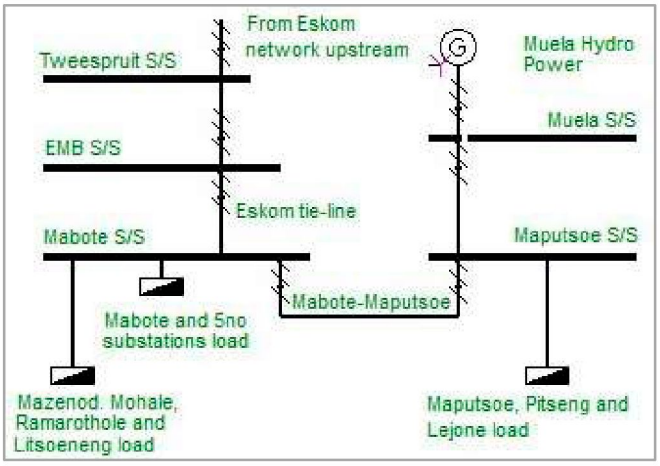

Fig. 3: The schematic diagram showing the part of the network that connects to Mabote substation

With reference to Table 1 with attention to the study cases 6 to 8, the simulations show that the system frequency recovered post the operation of stage 2 load-shedding (see Fig. 4). The important variables monitored were active power and reactive power, line-line voltage and excitation voltage. Taking study case 8 as the optimal solution, dropping 46.72 MW for stage 1 and allowed for 6.82 s time delay before activation of stage 2 resulted into a frequency fall to 47.0 Hz, frequency recovered on application of stage 2 load-shedding.

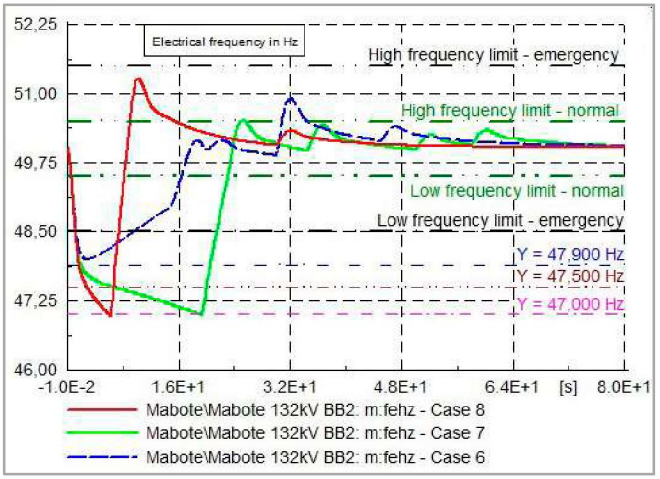

Fig. 4: Comparison of frequency (Hz) response for study cases 6 to 8

From Fig. 4, the activation of stage 2 resulted in fast frequency recovery because of dropping 29.53 MW, the recovery complied with the requirements of [7] for the frequency limits of 48.5 Hz to 47.5 Hz but violated 47 Hz limit (t<3.86 s) during emergency conditions. The Lesotho grid code does not specify the limits. Considering study case 8, in Fig. 5 to Fig. 7, the simulations showed compliance on the following post the dynamic load-shedding operation:

- The active power and reactive power was stable, but required another load-shedding stage to meet the operational reserve;
- Voltage was stable for emergency condition limits, and
- Excitation system settled down.

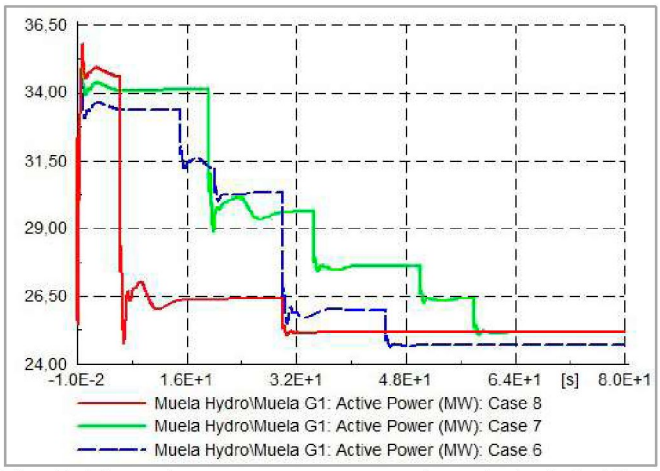

Fig. 5: The active power response to dynamic load-shedding operation for study cases 6 to 8

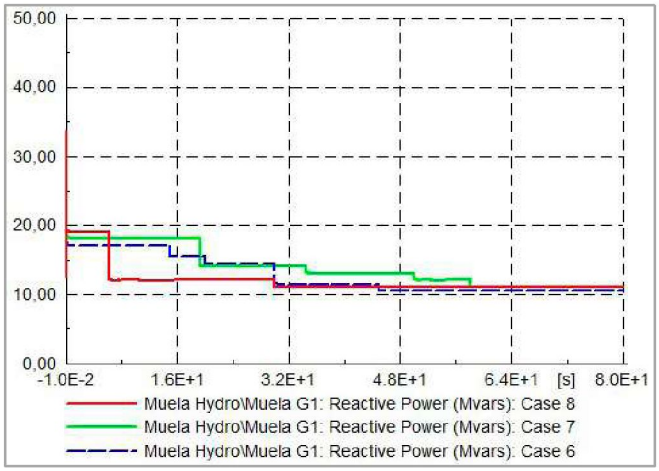

Fig. 6: The reactive power response to dynamic load-shedding operation for study cases 6 to 8

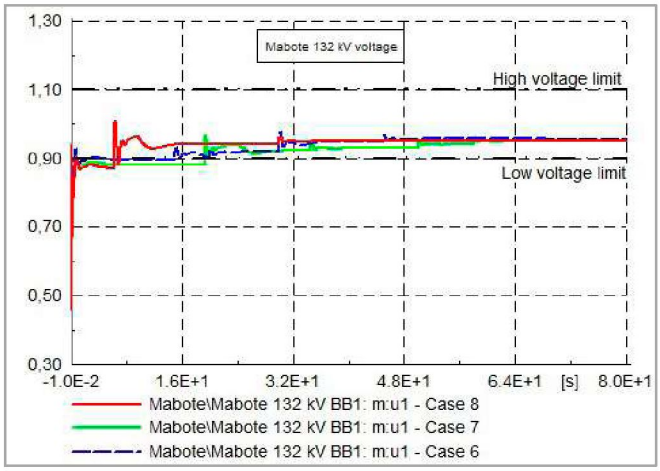

Fig. 7: The line-to-line voltage characteristics to dynamic load-shedding operation for study cases 6 to 8

IV. The Investigation of System Transient Stability

When faults occur on the system, they cause overloads, voltage violations, frequency violations and threaten the system stability if the protection system is not activated on time [1], [9]. The system stability is judged by the ability of

the generators to maintain synchronism during and / or after a faulted condition on the system [8, p. 47]. The loss of synchronism is an undesirable outcome owing to threats that come with out-of-step operation.

The generation and load mismatch during the fault condition initiate transients that cause the rotor to swing, because of the acceleration or braking torque applied on the rotor [9] [9]. In the perturbations, the breaker tripping operations clear faults and isolate the faulted section of the system.

Considering the faulted condition on the tie-line, a fault was applied on the transmission line at different locations to establish the critical fault clearing time (CFCT). In analyzing each case, the CFCT is important because it determines if the system is transiently stable. The computation of actual clearing time originates from Eq. (5) [9].

$$K_{time} = \frac{(t_{cr} - t_f)}{t_{cr}} \quad (5)$$

Where

t_{cr} is critical clearing time

t_f is actual clearing time

K_{time} is transient stability margin

From reference [10], the determination of system stability together with the computations of critical clearing angle δ_c follow Eq. (6).

$$\delta_c = \cos^{-1}\left\{\left|\frac{1}{r_1 - r_2}\right|\left[\left(\frac{P_m}{P_M}\right)(\delta_m - \delta_0)\right] + r_2\cos\delta_m - r_1\cos\delta_0\right\} \quad (6)$$

Where

P_M – peak pre-fault power angle curve

r_1 – peak of power angle curve ratio of the faulted circuit to P_M

r_2 - peak of power angle curve ratio to P_M with fault cleared

$$\delta_{0=\sin^{-1}\left(\frac{P_m}{P_M}\right)<\frac{pi}{2}}$$

$$\delta_{m=\sin^{-1}\left(\frac{P_m}{r_2 \times P_M}\right)>\frac{pi}{2}}$$

A. *Procedure for testing the contingencies*

The procedure for testing the contingencies was:

- A fault was applied on the line in the range of 5% to 95% of each line length at 100 ms;
- The line tripped at the substations at varying times until it reached and or exceeded the CFCT;
- The line tripped at node-j (j- denoting the other end of the faulted line) because of inter-trip activation;
- Calculation of the values for critical clearing times and critical clearing angle for both cases, and
- Identification of the system elements that were unstable.

B. *Critical fault clearing time (CFCT) application procedure*

The simulations of the faulted conditions in this study used the CFCT technique, which uses an iterative process [4]. In testing the transient stability limit, the focus was to determine the CFCT for different fault types on the critical transmission lines, viz. Tweespruit-EMB and Mabote-Maputsoe. The scenarios included a fault applied on line 1 when line 2 was in-service and a fault on line 1 when line 2 was out-of-service on both critical transmission lines.

The simulations' output included monitoring the dynamic variables and results thereof to assess the fault impact on the system. The monitored variables and their importance are:

- Active and reactive power – during island operation, the generators should operate within their capability limits to avoid unsafe operating area.
- Excitation voltage – changes the amount of reactive power produced which is necessary to maintain stable generator terminal voltage.
- Rotor angle of the generator –determines the amount of torque and the rotor current injection to maintain constant generator terminal voltage.
- Speed of the generator – provides an indication of the relationship between the generated active power and the load active power during islanding.
- Line-to-line voltage – is necessary for healthy operation of the equipment and loads connected to the system and for voltage compliance purposes.
- Phase currents – are necessary for determination of active power, voltage and load angle.

The study used the CFCT results to evaluate the requisite settings for zones 1 and 2 in view of the stability limitations.

1) *The three-phase fault on line 1 when line 2 was in-service*

The fault was applied individually on the line location as indicated on Fig. 8 for both Tweespruit-EMB and Mabote-Maputsoe transmission lines. Considering Tweespruit-EMB transmission line, from the results in Fig. 8, the typical zone 2 settings of 0.5 s is longer than the CFCT.

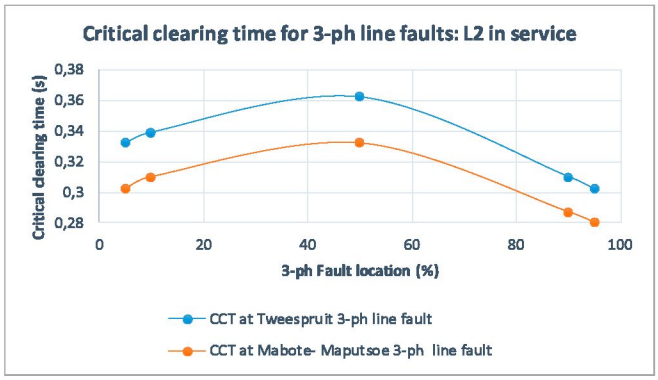

Fig. 8: The critical fault clearing time for a three-phase fault on the critical transmission lines

The simulation results using DIgSILENT indicate that the lowest CFCT of 0.302 s was reached for a faulted condition on 90% of the protected Tweespruit-EMB transmission line. These results for various fault location (see Fig. 8) show that

that loss of synchronism is eminent for settings with a longer time delay than the CFCT. Considering the Eq. (5), the decisions on settings should allow for a stability margin.

Taking a detailed look at a fault applied at 10% of the Tweespruit-EMB transmission line length, the CFCT was 0.34 s. With a fault applied at 100 ms from steady state, the CFCT occurred at 0.44 s. The stability was determined by adjusting the trip time from 0.44 s (CFCT), 0.45 s and 0.5 s to monitor the generator rotor angle on fault application. The results show that the system was stable up to 0.44 s (the CFCT) and pole-slipped on application of 0.45 s fault clearing time (see Fig. 9).

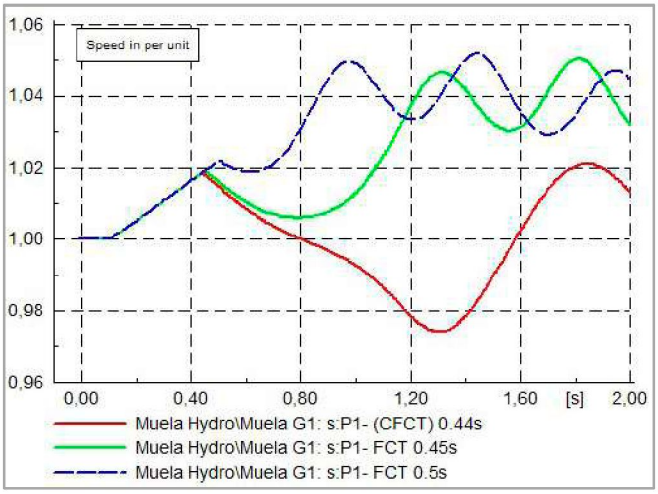

Fig. 9: Generator speed characteristic showing out-of-step condition for fault clearance time exceeding the CFCT

2) The three-phase fault on line 1 when line 2 was out-of-service

Considering maintenance on either line and that the faults happen abruptly, a severe three-phase fault was applied on both the critical transmission lines independently on different line fault locations (see Fig. 10.). The procedure stated in section IV, 'A' was followed. Because of line 2 being out-of-service, the overall system impedance increased hence the increased stability margin for this contingency. The simulations showed that for the faulted condition at 10% of Tweespruit-EMB and Mabote-Maputsoe transmission lines lengths, the CFCT was 1.119 s and 0.988 s respectively.

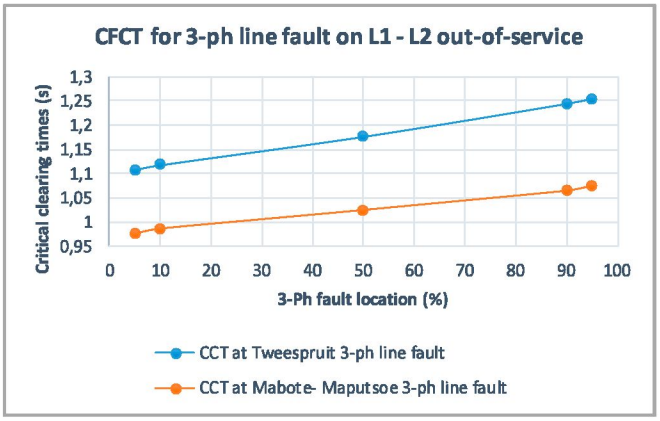

Fig. 10: The critical fault clearing time for a three-phase fault on the critical transmission lines

For faults close to the Eskom side of these lines with the second line out of service, resulted in:

- Voltage suppression at all substations (see Fig. 11);
- Generators losing synchronism when running at 107% of the rated speed, and
- The transmission line was operating at a higher load than 60 MW surge impedance loading.

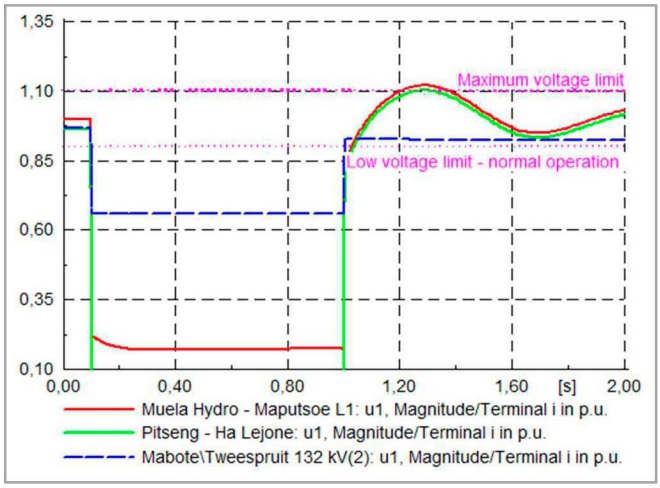

Fig. 11: A voltage response to a three-phase fault with line 2 out-of-service

3) The three-phase fault on Mabote 33/11 kV busbars

The substations connecting directly to Mabote substation supply approximately 44.54 MW. This constitute ±30% of the total Lesotho power system load (see Fig. 3) making an investigation into impact that each fault type puts on the system very important.

The transient stability was tested through the application of a three-phase fault on Mabote 11 kV and 33 kV busbars following the procedure in section IV, 'A'. Different considered fault types were three-phase, phase-phase, and single-phase-to-ground faults. Of all these faults, only the three-phase fault on the 33 kV busbars resulted in system frequency instability (see Table 2).

Table 2: The transient stability results for Mabote 33/11 kV busbars

Fault type	*Location*	*Critical clearing time (s)*	*Frequency stability*	*Voltage status*
3-ph	Mabote 33 kV BB	1.442 s	Unstable	Unstable
2-ph-G	Mabote 33 kV BB	N/A	Stable	Unstable
1-ph - G	Mabote 33 kV BB	N/A	Stable	Unstable
3-ph	Mabote 11 kV BB	N/A	Stable	Unstable
2-ph-G	Mabote 11 kV BB	N/A	Stable	Unstable
1-ph - G	Mabote 11 kV BB	N/A	Stable	Unstable

V. INVESTIGATION OF POSSIBLE SVC INSTALLATION IMPACT

Bearing in mind both active and reactive power oscillations occur during the re-energizing, the amplitude of power oscillations beyond the generators' ratings warranted an investigation into the impact a static var compensator (SVC) would have on the LPS. The advantage of installation was improved voltage control, because of being an additional source while the drawback was a reduced stability margin (see Fig. 12).

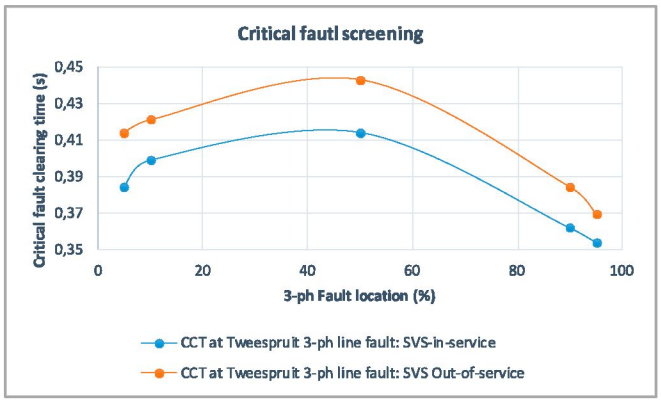

Fig. 12: Impact of SVC installation on the critical fault clearing time

VI. Analysis of System Behavior During Synchronizing

Since 1998 when 'Muela hydro-power was commissioned, the load on the LPS has increased. In 2016, the peak load demand was 150 MW because of an increased industrial activity and commercial developments. With no dynamic load curtailment to permit islanding during emergency conditions, the supply /demand balance accuracy remain fragile.

The status quo is that the system does not resynchronize to the grid assuming a successful island operation. To reconnect the two systems, 'Muela hydro-power generators trip and are resynchronized after the grid picked-up the load. This paper further investigated the causes and factors that contribute to the tie-line breaker's failure to close. Using [2] as a guide on the requisite limits for the breaker closing angle, voltage difference between the two systems and frequency difference as $\pm 10^0$, 0% to +5% and 0.067 Hz, the system was tested on at these conditions to establish the extreme limits within which breaker closure was successful (see Table 3).

Table 3: The summary of the load condition impact for the requisite tie-breaker closing conditions

Pre-switching load (MW)	*Rotor angle max (deg.)*	*Peak power swing (MW)*	*% change in frequency*	*% system overload*	*Breaker angle at Mabote*
24,103	36,713	30,602	0,50%	100,20%	-9,66
25,14	47,713	33,291	0,80%	105,30%	-10,107
25,791	51,303	35,031	1,00%	108,60%	-10,397
26,228	53,84	36,197	1,10%	111,00%	-10,598
26,516	55,539	36,903	1,20%	111,90%	-10,689
26,595	55,975	37,103	1,20%	112,00%	-10,689
26,636	56,291	37,22	1,20%	112,30%	-10,765
26,847	56,291	40,369	1,30%	113,90%	-10,842

In performing the load tests prior to resynchronizing, the impact of the peak power swing was evaluated through switching different combinations of loads. Contrary to the recommendations in [1], the 1.5 per unit limit was increased to 1.55 per unit beyond which the generating units were unstable upon closing the tie-line breaker. The next sections discuss the impact that each variable had on the breaker closing operation.

A. *Breaker voltage angle variations across the open-poles*

The relationship between the loading condition and the breaker voltage angle show that the limits provided in [1], [3] can be exceeded. Thus, further increase in load is indirectly proportional to the chances of success on closing the tie-line breaker. From Table 3, the breaker angle difference was enlarged from 10° to 10.77° and a function of load on the system. Further increases in load resulted in an unstable system (see Fig. 13).

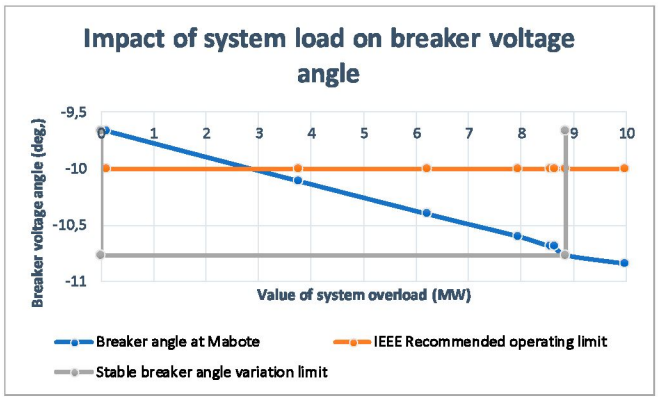

Fig. 13: The system overload limits to permit safe tie-line breaker closing

B. *Voltage difference between the two systems*

From Table 3, the voltage variations were within the recommended limits in [3],[8] for different permissive breaker close requirements. The reduced voltage variation is important for improved power system stability by permitting the reactive power into the system [8].

C. *Frequency variations*

Different to the recommendations in [2], the simulations' results show that synchronizing is permissive above the 0.067 Hz up to 0.6 Hz for increasing system load conditions (see Fig. 14). Reference [8] characterizes large frequency differences to rapid load pickup or even excessive machine motoring mode operation.

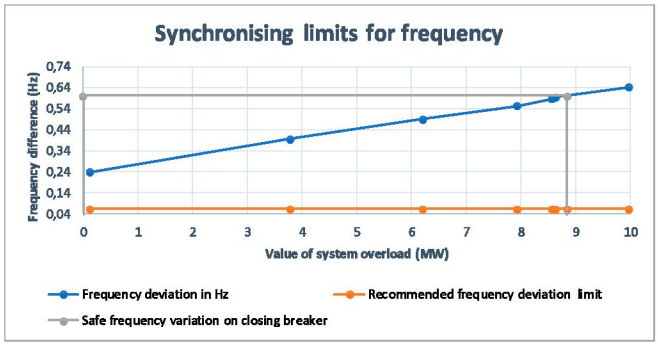

Fig. 14: The frequency variation limit for safe breaker closing into synchronism

D. *Peak active power swing limit on closing the tie-line breaker*

Divergent to the limits in [1], the simulation results show that the peak active power swing oscillated back in to stable condition with the maximum rotor angle oscillations swing of 56.3°. From Fig. 15, the results further show that the peak active power swing permits stable operation including 100%

to 155% of the generator rated capacity with progressively reducing chances of success.

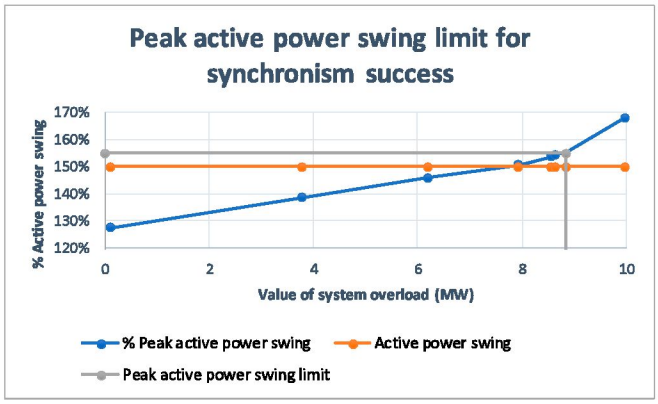

Fig. 15: Peak active power swing limit for successful synchronizing

VII. Impact of different power Load restoration on the system

The load restoration was tested considering two scenarios, viz. restoring the all loads shed in hypothetically one switching action versus restoring in small blocks. The simulations show that the two scenarios had minimal impact on the generators (see Fig. 16). In practice, the operators restore loads through switching one breaker load at the time.

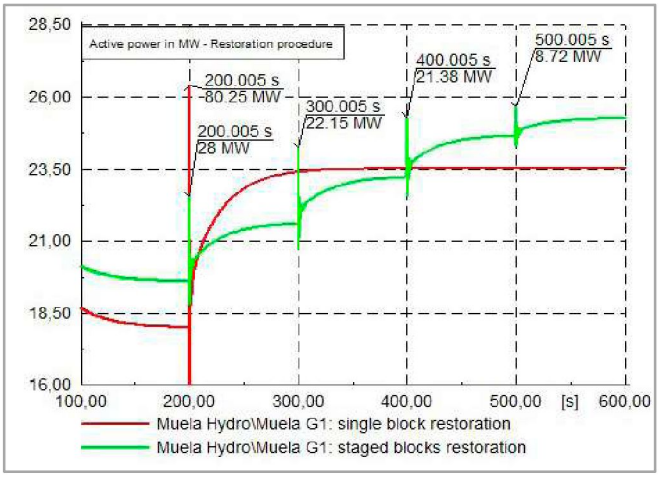

Fig. 16: Comparison of the impact of restoring different amounts of load on the generating units

VIII. Conclusion

The outcome of this study provides valid solutions achieved through use of DIgSILENT for system modelling.

Application of dynamic load-shedding during perturbations that cause power transfer failure to the Lesotho power system can solve the causes of system collapse during loading more than the installed generators' rating.

The transient stability is reached with the application of faults with clearing times of 300 ms and 280 ms respectively for the Tweespruit-EMB and Mabote-Maputsoe transmission lines with both lines in-service.

The installation of an SVC to absorb power oscillations during the perturbations can also improve the voltage stability. However, the drawbacks of this solution include reduced stability margin.

The study established the limits for successful re-synchronizing with the associated variances in the voltage load angle, system load, frequency, and peak active power swing.

Loads restoration in any sequence does not compromise the generators' operating limits.

IX. Bibliography

[1] IEEE Transactions on Power Apparatus and systems, "EEE Screening guide for planned steady state switching operations to minimize harmful effects on steam turbine-generators," IEEE, 1980.

[2] IEEE Power and Energy Society, "IEEE Standard for Cylindrical-Rotor 50 Hz and 60 Hz Synchronous Generators rated 10 MVA and above," IEEE Standards Association, New York, 2014.

[3] IEEE Power and Energy Society, "IEEE Standard for Cylindrical-Rotor 50 Hz and 60 Hz Synchronous Generators rated 10 MVA and Above," IEEE-SA Standard Board, New York, USA, 2014.

[4] DIgSILENT PowerFactory 15, Technical Reference Documentation - Complex Load, Gomaringen, Germany: DIgSILENT GmbH, 2014.

[5] D. G. Chown, Writer, *Network Frequency Control with Increasing Renewable Power Plants. SAIEE course notes*, 2014.

[6] Economic Consulting Associates Limited, "South African Power Pool (SAPP) | Transmission & Trading Case Study," Economic Consulting Associates, London, 2009.

[7] The South African Grid Code – Network Code, "The South African Grid Code – Network Code," The South African Grid Code – Network Code, 2008.

[8] IEEE Power Engineering Society, "IEEE Guide for AC Generator Protection," IEEE, New York, 2006.

[9] J. G. Duncan, S. S. Mulukutsa and J. O. Thomas, Power system analysis and design, Stamford: Engage Learning, USA, 2012.

[10] P. A. A. Fouad, Power System Control and Stability, California: A John Wiley and Sons, Inc., 2003.